Int. J. Heat Mass Transfer. Vol. 27, No. 3, pp. 391–398, 1984
Printed in Great Britain

0017 9310/84 $3.00 + 0.00
Pergamon Press Ltd.

LAMINAR HEAT TRANSFER TO BLOOD FLOWING IN A CIRCULAR DUCT

ANTONIO DUMAS and GIOVANNI S. BAROZZI
Istituto di Fisica Tecnica, Università di Bologna, V. le Risorgimento, 2—I-40136 Bologna, Italy

(*Received* 30 *March* 1983)

Abstract—Entrance-region heat transfer to blood steadily flowing in a pipe is studied. It is assumed that the non-Newtonian behaviour of blood can be expressed both by the Casson equation and the more complex law suggested by Merrill and Pelletier [*J. Appl. Physiol.* **23**, 179–182 (1967)]. The possible presence of a thin cell-free plasma layer at the wall is accounted for. The velocity distribution is determined analytically and a solution of the energy equation is obtained by a finite-difference method, for the two cases: (a) the uniform wall temperature, and (b) the uniform wall heat flux. Results are presented for the yield number $Y\ (= 2R\tau_y/\sigma u_m) = 1$, 5, 10 and 20 and the non-dimensional marginal layer thickness $D\ (= \delta/R) = 0$, 0.0002, 0.01 and 0.1.

NOMENCLATURE

a_1, a_2, a_3 dimensional constants in equation (3)
b_1, b_2 non-dimensional constants in equation (18)
c_1, c_2 non-dimensional constants in equation (19)
c specific heat
D non-dimensional thickness of the plasma layer, δ/R
F non-dimensional pressure gradient parameter, $|dp/dx'|4R^2/\sigma u_m$
Ⓗ thermal boundary condition referring to constant heat flux at the wall
h convective heat transfer coefficient
K non-dimensional thermal conductivity, k_p/k_b
k thermal conductivity
M non-dimensional thermal diffusivity, $k_p\rho_b c_b/k_b\rho_p c_p$
Nu Nusselt number, $h2R/k_b$
P non-dimensional viscosity, μ_p/σ
p pressure
Pe Péclet number $2Ru_m\rho_b c_b/k_b$
q wall heat flux
R radius of the pipe
r' radial coordinate
r non-dimensional radial coordinate, r'/R
T temperature
Ⓣ thermal boundary condition referring to constant wall temperature
u' fluid axial velocity
u non-dimensional fluid axial velocity, u'/u_m
x' axial coordinate
x^* non-dimensional axial coordinate, $x'/2R\ Pe$
Y yield number, $2R\tau_y/\sigma u_m$.

Greek symbols

α, β dimensional constants in equation (3)
γ rate of strain
δ thickness of the marginal plasma layer
θ non-dimensional fluid temperature, $(T-T_0)/qRk_b^{-1}$ for case Ⓗ and $(T-T_0)/(T_w-T_0)$ for case Ⓣ
μ dynamic viscosity coefficient
ρ density of the fluid
σ dimensional constant in equations (2) and (3)
τ shear stress
τ_y yield stress.

Subscripts

b blood
CL centre line
H referring to condition Ⓗ
m mean value
0 at the inlet section
p plasma
w at the wall
x local value
T referring to condition Ⓣ
δ at the plasma–blood interface.

INTRODUCTION

VERY accurate control of the temperature and heat flux is demanded in operating extracorporal devices, such as oxygenators and artificial kidneys. Consequently profound knowledge of the thermophysical properties and their influence on the fluid-dynamic and thermal behaviour of blood is needed to design and develop such equipment.

Whole blood essentially consists of a suspension of red cells and other formed elements of a smaller size in a continuous medium termed plasma. The assumption of a Newtonian homogeneous fluid may then be too approximate for this very complex structure.

In fact several *in vivo* and *in vitro* experiments, quoted by Cooney [1], have shown the presence of a 3–5 μm thick cell-free plasma layer at the periphery of the vessels. Furthermore, viscosimetric results have demonstrated that the rheological behaviour of blood is characterized by the existence of a yield stress and a non-linear shear stress–shear rate relationship, as expressed in the rheological models due to Charm and Kurland [2] and Merrill and Pelletier [3]. These effects may cause the asymptotic velocity distribution to deviate from the well-known Hagen–Poiseuille con-

figuration, as the computations performed by Merrill *et al.* [4] and Salvigni *et al.* [5] have shown.

The related consequences on the heat transfer to blood flow were first studied by Mitvalsky [6] and Charm *et al.* [7].

Mean values of the Nusselt number for the boundary condition of constant temperature at the wall were obtained for diluted and undiluted blood as well as for plasma. However, probably due to experimental difficulties, the results offer no conclusive information.

Victor and Shah [8, 9] have accounted for the non-Newtonian behaviour of the blood dealing with the theoretical determination of the convective heat transfer coefficients in pipe flow. The asymptotic values of the local Nusselt number either for the boundary condition of constant temperature Ⓣ or of uniform flux at the wall Ⓗ are given in ref. [8], where blood is treated as a Casson fluid as suggested by Charm and Kurland [2]. The velocity profiles were determined by the analytical method of Merrill *et al.* [4].

The investigation was then extended to cover the dynamic and thermal entrance region [9], using the numerical method of Patankar and Spalding [10].

Assuming the Charm and Kurland model [2] and accounting for the presence of a cell-free plasma layer at the wall Zanchini *et al.* [11] have studied the asymptotic thermal behaviour of blood flowing in vessels.

In this paper the thermal inlet region of blood flowing in a pipe is analysed for the Ⓣ or Ⓗ boundary condition keeping in mind the possible presence of a thin plasma layer at the wall. Either the Charm and Kurland relationship or the more refined model proposed by Merrill and Pelletier is utilized to characterize the rheological behaviour of the blood.

GOVERNING EQUATIONS AND PROCEDURE

Velocity distribution

As long as a fully developed axisymmetric flow of a constant-property fluid is considered, the conservation equations of mass and momentum give

$$\tau = -\frac{\mathrm{d}p}{\mathrm{d}x'}\frac{r'}{2}. \tag{1}$$

The dynamical problem must be completed by defining the shear stress–shear rate relationship and imposing the usual no-slip condition for velocity at the wall.

According to the Charm and Kurland model, here denoted as model A, the blood can be represented rheologically as a Casson fluid

$$\begin{aligned} \gamma \equiv \frac{\mathrm{d}u}{\mathrm{d}r'} = 0 \qquad & \text{for} \quad \tau \leqslant \tau_y, \\ \sqrt{\tau} = \sqrt{\tau_y} + \sqrt{(\sigma\gamma)} \quad & \text{for} \quad \tau \geqslant \tau_y. \end{aligned} \tag{2}$$

Following the model suggested by Merrill and Pelletier, model B, the constitutive equation is expressed as

$$\begin{aligned} \gamma &= 0 && \text{for} \quad \tau \leqslant \tau_y, \\ \sqrt{\tau} &= \sqrt{\tau_y} + \sqrt{(\sigma\gamma)} && \text{for} \quad \tau \geqslant \tau_y \quad \text{and} \quad \gamma \leqslant \alpha, \\ \sqrt{\tau} &= \sqrt{a_1} + \sqrt{(a_2\gamma)} && \text{for} \quad \alpha \leqslant \gamma \leqslant \beta, \\ \tau &= a_3\gamma && \text{for} \quad \gamma \geqslant \beta. \end{aligned} \tag{3}$$

The plasma in the marginal cell-free layer is always assumed to be Newtonian with a constant viscosity coefficient μ_p.

The values of the yield stress τ_y, the empirical constants in the foregoing relationships and other thermophysical quantities are given in Table 1.

From dimensional analysis considerations the velocity distribution is found to be dependent on three non-dimensional groups whichever model is used: the yield stress number Y, the marginal layer thickness D, the viscosity ratio P, defined respectively as $Y = (2R\tau_y/\sigma u_m)$, $D = \delta/R$, $P = \mu_p/\sigma$.

The fourth non-dimensional group, the pressure gradient parameter, resulting in equations (4)–(11) is, on the contrary, a dependent variable. It is defined as

$$F = \left|\frac{\mathrm{d}p}{\mathrm{d}x'}\right| 4R^2/\sigma u_m.$$

The flow field for model A is described by the following non-dimensional relationships

$$u_3 = F(1-r^2)/(16P) \quad \text{if} \quad r_\delta \leqslant r \leqslant 1, \tag{4}$$

$$u_2 = u_3(r_\delta) + F(r_\delta^2 - r^2)/16 + Y(r_\delta - r)/2 - (FY)^{1/2}(r_\delta^{3/2} - r^{3/2})/3 \quad \text{if} \quad r_1 \leqslant r < r_\delta, \tag{5}$$

$$u_1 = u_2(r_1) \quad \text{if} \quad r \leqslant r_1, \tag{6}$$

here $r_\delta = 1 - D$ and $r_1 = 4Y/F$.

According to model B five flow regions must in general be considered and the velocity distribution is expressed by

$$u_5 = F(1-r^2)/16P \quad \text{if} \quad r_\delta \leqslant r \leqslant 1, \tag{7}$$

$$u_4 = u_5(r_5) - F(r^2 - r_\delta^2)/16A_3 \quad \text{if} \quad r_3 \leqslant r \leqslant r_\delta, \tag{8}$$

$$u_3 = u_4(r_3) + F(r_3^2 - r^2)/16A_2 + A_1Y(r_3 - r)/2A_1 - (A_1FY)^{1/2}(r_3^{3/2} - r^{3/2})/6A_2 \quad \text{if} \quad r_2 \leqslant r \leqslant r_3, \tag{9}$$

$$u_2 = u_3(r_2) + F(r_2^2 - r^2)/16 + (r_2 - r)/2 - (FY)^{1/2}(r_2^{3/2} - r^{3/2}) \quad \text{if} \quad r_1 \leqslant r \leqslant r_2, \tag{10}$$

$$u_1 = u_2(r_1) \quad \text{if} \quad r \leqslant r_1, \tag{11}$$

where $A_1 = a_1/\tau_y$, $A_2 = a_2/\sigma$, $A_3 = a_3/\sigma$, $r_1 = 4Y/F$, $r_2 = (4YA_1/F)^{1/2} + (8A_2\gamma_2/F)$, $r_3 = 8A_3\gamma_3/F$, $\gamma_2 = \alpha u_m/R$, and $\gamma_3 = \beta u_m/R$.

To determine the velocity distribution the iterative procedure suggested in ref. [5] is employed: for assigned values of Y and D, P being always held constant, a guess value of F is used to obtain the mean velocity. The corresponding value of the yield number is compared with the original one and, using a simple trial and error technique, a new run starts if the prefixed convergency level is not reached. The fluid velocity can

Table 1. Properties of blood and plasma (from refs. [2, 3, 9, 11])

Whole blood	$k_b = 0.505$ W m^{-1} K^{-1};	$c_b = 3.85$ kJ kg K^{-1}
	$\rho_b = 1055$ kg m^{-3}	
Model A	$\tau_y = 1.09 \times 10^{-2}$ N m^{-2};	$\sigma = 2.76 \times 10^{-3}$ N s m^{-2}
Model B	$\tau_y = 2.25 \times 10^{-3}$ N m^{-2};	$\sigma = 2.99 \times 10^{-3}$ N s m^{-2}
	$a_1 = 6.85 \times 10^{-3}$ N m^{-2};	$a_2 = 2.40 \times 10^{-3}$ N s m^{-2}
	$\alpha = 31.5$ s^{-1}; $\beta = 100$ s^{-1};	$a_3 = 3.24 \times 10^{-3}$ N s m^{-2}
Plasma	$k_p = 0.582$ W m^{-1} K^{-1};	$c_p = 3.94$ kJ kg^{-1} K^{-1}
	$\rho_p = 1035$ kg m^{-3};	$\mu_p = 1.5 \times 10^{-3}$ N s m^{-2}

then be computed by the equations related to the model used.

Energy equation

Disregarding axial fluid conduction, internal heat generation and dissipation, the two energy balance equations to be written for blood and for plasma may be collected in a single non-dimensional form

$$4M \frac{1}{r} \frac{\partial}{\partial r}\left(r \frac{\partial \theta}{\partial r}\right) - u \frac{\partial \theta}{\partial x^*} = 0, \tag{12}$$

where the parameter $M = (k_p/\rho_p c_p)/(k_b/\rho_b c_b)$ is present only in the expression of the energy equation regarding the plasma region.

The non-dimensional temperature is defined for the uniform heat flux as

$$\theta = \frac{T - T_0}{qR/k_b},$$

or, for the uniform wall temperature, as

$$\theta = \frac{T - T_0}{T_w - T_0}.$$

A statement of the problem is accomplished by the following sets of conditions:

$$\begin{aligned} &\theta = 0 \quad \text{for} \quad x^* = 0, \\ &\frac{\partial \theta}{\partial r} = 0 \quad \text{for} \quad r = 0, \\ &\frac{\partial \theta}{\partial r} = K \quad \text{or} \quad \theta = 1 \quad \text{for} \quad r = 1, \end{aligned} \tag{13}$$

and

$$\begin{aligned} &K \left.\frac{\partial \theta}{\partial r}\right|_{r^+} = \left.\frac{\partial \theta}{\partial r}\right|_{r^-} \quad \text{for} \quad r = r_\delta, \\ &\theta|_{r^+} = \theta|_{r^-}, \end{aligned} \tag{14}$$

here $K = k_p/k_b$.

The new parameters M and K, derived from the non-dimensionalizing process, complete the set of independent non-dimensional groups of the problem.

Besides the temperature distribution of the fluid, the bulk temperature and local and mean values of the Nusselt number are of engineering interest. They are defined as follows

$$\theta_m = \frac{\int_0^{r_\delta} u0r \, dr + (\rho_p c_p/\rho_b c_b) \int_{r_\delta}^1 u0r \, dr}{\int_0^{r_\delta} ur \, dr + (\rho_p c_p/\rho_b c_b) \int_{r_\delta}^1 ur \, dr}, \tag{15}$$

$$Nu_x = \frac{2(\partial\theta/\partial r)_{r=1}}{\theta_w - \theta_m} K, \tag{16}$$

$$Nu_m = \frac{1}{x^*} \int_0^{x^*} Nu_x \, dx^*. \tag{17}$$

Numerical method

A finite-difference procedure is used to solve equations (12)–(14).

The scheme is derived from the fully implicit numerical method widely described in ref. [12] and utilized in ref. [13] where the Graetz problem with axial fluid conduction was considered. Due to the parabolic structure of the energy equation a simplified version is used here.

As a first step a variable size mesh is built up on the domain of integration. This is achieved by assigning constant increments to the auxiliary variables (η, ρ) defined by the equations

$$\eta = \tanh [b_1 x^{*b_2}] \quad \text{for} \quad 0 < x^*, \tag{18}$$

$$\rho = c_1 r^2 + c_2 r \quad \text{for} \quad 0 < r < 1, \tag{19}$$

where b_1, b_2, c_1, and c_2 are constants whose values can be suitably chosen to fit the physical problem studied.

The coordinates of the grid points (x_i^*, r_j) are obtained by the inverse transformations of equations (18) and (19).

A central difference is used to discretize the first term in equation (12) while the convective term is replaced with a backward difference. The resulting algebraic linear equation is

$$\begin{aligned} 4M \Bigg(&\frac{1}{r_j} \frac{\theta_{i,j+1} - \theta_{i,j-1}}{r_{j+1} - r_{j-1}} \\ &+ 2 \frac{(r_j - r_{j-1})\theta_{i,j+1} - (r_{j+1} - r_{j-1})\theta_{i,j} + (r_{j+1} - r_j)\theta_{i,j-1}}{(r_j - r_{j-1})(r_{j+1} - r_{j-1})(r_{j+1} - r_j)} \\ &- u_j \frac{\theta_{i,j} - \theta_{i-1,j}}{x_i^* - x_{i-1}^*} \Bigg) = 0. \end{aligned} \tag{20}$$

If the radial coordinate value of the plasma–blood interface, r_δ, is comprised between r_{j-1} and r_{j+1}, the foregoing equation must be modified to account for the discontinuity of the temperature gradient. Fictitious nodal points (x_i^*, r_δ) are defined where the compatibility conditions (14) are imposed so that the following work expressions for the dependent variable at r_δ are obtained

$$\theta_{i,\delta} = \frac{K(r_\delta - r_j)\theta_{i,j+1} + (r_{j+1} - r_\delta)\theta_{i,j}}{K(r_\delta - r_j) + (r_{j+1} - r_\delta)} \quad \text{if} \quad r_j < r_\delta \leqslant r_{j+1}, \quad (21)$$

$$\theta_{i,\delta} = \frac{K(r_\delta - r_{j+1})\theta_j + (r_j - r_\delta)\theta_{i+1}}{k(r_\delta - r_{j+1}) + (r_j - r_\delta)} \quad \text{if} \quad r_{j-1} < r_\delta < r_j. \quad (22)$$

According to whether the central nodal point position belongs to the plasma or blood region, equations (21) and (22) respectively replace $\theta_{i,j+1}$ or $\theta_{i,j-1}$ in equation (20) and r_{j+1} or r_{j-1} must be substituted by r_δ.

The boundary conditions (13) are treated in a straightforward way and need not be discussed. Solution of the resulting system of equations is obtained by the Gauss elimination method with partial pivoting.

The presence of the plasma–blood interface, the variable step mesh used and the parabolic structure of the energy equation may cause large differences in the values of the matrix coefficients, so that significant information may be irretrievably lost through the need to truncate the sums to the available number size of the computer, the effect growing as the number of equations increases. This situation of artificial skewness may be detected and rectified by equilibrating the coefficient matrix. This can be achieved by transforming the primary system

$$\tilde{A}\tilde{T} = \tilde{B},$$

into a new one

$$\tilde{L}_2\tilde{A}\tilde{L}_1\tilde{T}_1 = \tilde{B}.$$

There are no general rules for the selection of $\tilde{L}_1$ and $\tilde{L}_2$ and only some suggestions based on empirical criteria can be found in refs. [14, 15]. In this work $\tilde{L}_1$ is a unitary squared matrix and $\tilde{L}_2$ a diagonal squared matrix whose elements are defined by

$$l_{ii} = 1/\Sigma_j |a_{ij}|.$$

This selection has proven to be fruitful in all the cases considered.

RESULTS AND COMMENTS

As a preliminary test, solution of the Graetz problem has been got and the results checked with the tabulated data referred by Shah and London [16]. Excellent agreement is found both for the Ⓣ and Ⓗ condition in the thermal inlet region.

The asymptotic values of the Nusselt number for a homogeneous Casson fluid have been compared with the analytical results of Victor and Shah [8] and a maximum deviation of 0.25% is observed. The fully developed temperature distributions have also been computed by the formulas derived in ref. [8] for the constant heat flux case.

Numerical and analytical results in the zones nearest the wall agree up to four digits, the deviation increasing to 2% on approaching the centre line of the tube. As already discussed in ref. [12] this trend is due to the non-uniform size of the grid. However, the accuracy of the results may be improved by tightening the meshes of the net.

Table 2. Centre line velocity and asymptotic values of the Nusselt number for all the cases considered

		Model A			Model B		
D	Y	u_{CL}	Nu_T	Nu_H	u_{CL}	Nu_T	Nu_H
0.0	1	1.784	3.802	4.547	1.889	3.687	4.379
	5	1.620	3.973	4.739	1.788	3.800	4.540
	10	1.539	4.060	4.883	1.724	3.851	4.603
	20	1.458	4.209	5.078	1.651	3.925	4.689
2×10^{-4}	1	1.782	3.854	4.599	1.888	3.740	4.337
	5	1.617	4.016	4.795	1.786	3.851	4.595
	10	1.534	4.129	4.943	1.722	3.903	4.656
	20	1.452	4.271	5.143	1.647	3.982	4.751
0.01	1	1.704	4.000	4.816	1.833	3.880	4.654
	5	1.482	4.898	5.231	1.700	4.009	4.835
	10	1.361	4.525	5.572	1.616	4.102	4.967
	20	1.232	4.852	6.036	1.514	4.252	5.164
0.1	1	1.375	4.666	5.862	1.560	4.370	5.423
	5	1.136	5.287	6.783	1.358	4.707	5.927
	10	1.105	5.408	6.981	1.250	4.951	6.273
	20	1.105	5.409	6.982	1.154	5.229	6.669

Final computations have been performed on a Vax 11/780 computer using a 20×40 grid. The constant b_1 is chosen in such a way that the first axial station is positioned at $x^* < 1 \times 10^{-6}$, as $0.3 \leqslant b_2 \leqslant 0.4$, $c_1 = 1$ and $c_2 = 0$ in equations (18) and (19). The values assigned to the non-dimensional groups D and Y are: $D = 0$, 0.0002, 0.01, 0.1; $Y = 1$, 5, 10, 20; all other parameters being held constant at the value computed from the data given in Table 1.

Owing to the different structures of the rheological models, equal values of Y should not correspond to physically comparable situations, so that, for both models, Y has been calculated by assuming the same diameter to mean velocity ratio and keeping for τ_y/σ the value corresponding to model A.

The asymptotic Nusselt number and the centre line velocity u_{CL} are given in Table 2 for all the cases considered.

In Figs. 1–3 some results are given in terms of local and mean Nusselt numbers against the non-dimensional distance from the inlet, x^*.

The influence of the non-Newtonian character of the blood always consists of an increase in the heat transfer rate. As long as the marginal cell-free layer is overlooked deviation from the Newtonian behaviour is not large and, furthermore, small differences are observed between the rheological models.

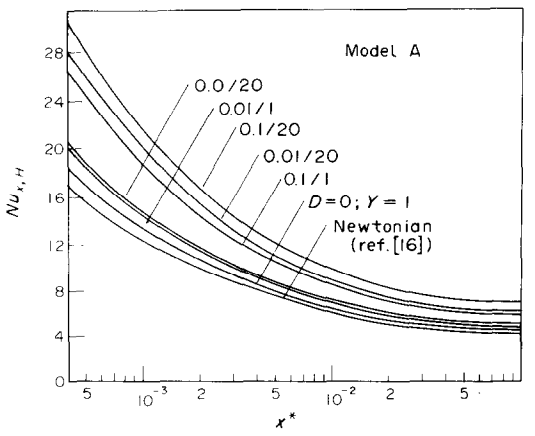

FIG. 1(a). Local Nusselt number vs downstream distance for the constant heat flux case, model A.

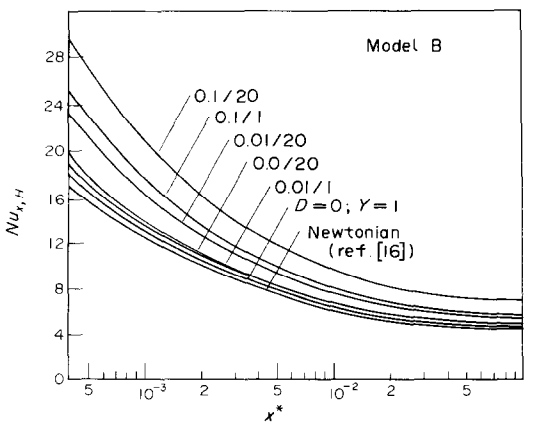

FIG. 1(b). Local Nusselt number vs downstream distance for the constant heat flux case, model B.

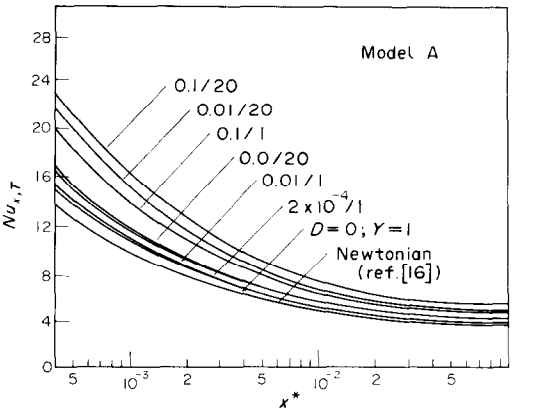

FIG. 2(a). Local Nusselt number vs downstream distance for the constant temperature case, model A.

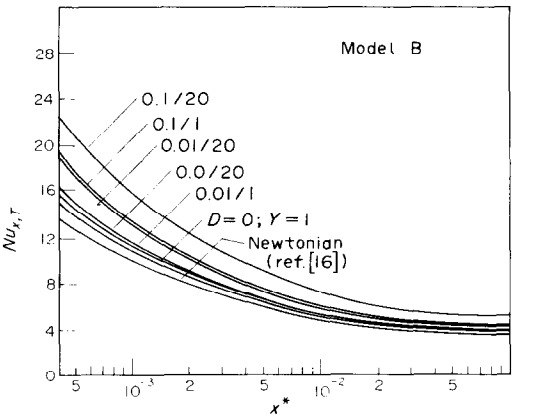

FIG. 2(b). Local Nusselt number vs downstream distance for the constant temperature case, model B.

As the thickness of the marginal plasma layer grows, higher values of the Nusselt number are found and the effect of the yield number becomes more pronounced. The same trend is found with both rheological models used.

It is noticed that higher values of the Nusselt number are always obtained with model A than with model B at equal values of D and Y and, moreover, the results are more sensitive to variations in plasma layer thickness and yield number. This effect is better displayed in Fig. 4 where for all the runs performed with condition Ⓗ, Nu_x is plotted vs Y on the same abscissa, $x^* = 0.98 \times 10^{-2}$.

This trend may be understood by observing the velocity profiles with and without the plasma layer, at different values of Y and D in Fig. 5.

As already discussed by Victor and Shah [8, 9] for a homogeneous Casson fluid, the presence of a plug-like flow in the stream core is responsible for the increase in

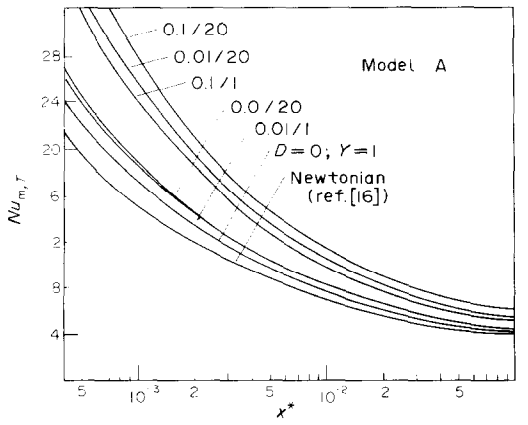

FIG. 3(a). Mean Nusselt number vs downstream distance for the constant temperature case, model A.

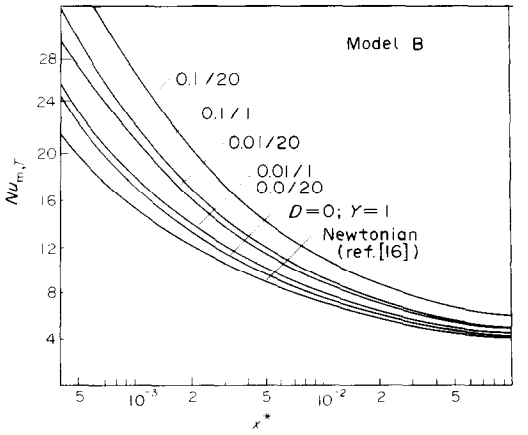

FIG. 3(b). Mean Nusselt number vs downstream distance for the constant temperature case, model B.

the Nusselt number compared with that of a Newtonian fluid. This behaviour is confirmed here also when a thin plasma layer is considered. In fact, plasma, compared with whole blood, has a considerably lower apparent viscosity, so that its presence modifies the velocity gradient at the wall, reduces centre line velocity

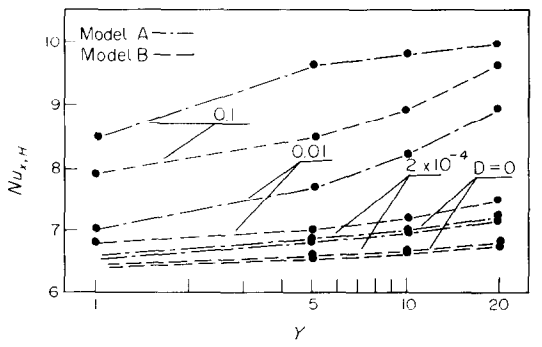

FIG. 4. Local Nusselt number vs yield number for $x^* = 0.98 \times 10^{-2}$.

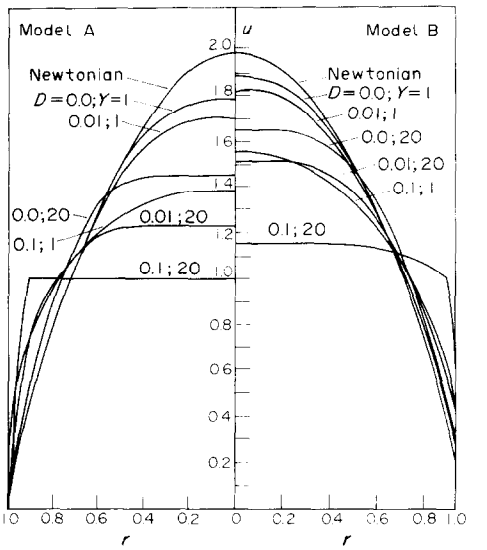

FIG. 5. Fully developed velocity profiles for blood flow in a pipe.

and, correspondingly, the plug flow region broadens further on.

The fundamental importance of velocity distribution on the heat transfer rate could lead to the belief that more relevant effects should be found in a hydrodynamic developing flow region. Nevertheless due to the rather high Prandtl number of the blood, $Pr \cong 25$, the hydraulic entrance region should be very short, so that no significant difference should be found some diameters after the inlet section.

This is confirmed, at least in the absence of the plasma layer, by the very good agreement between Victor and Shah's results [9] for a developing Casson fluid flow and the corresponding data presented here for model A, referring to the thermal inlet region.

CONCLUDING REMARKS

So far as we know there is no known solution available for heat transfer in the thermal entrance region for a fluid which obeys the Casson stress–strain relationship or a more refined model with or without the presence of a Newtonian fluid layer at the wall. Having confirmed that these results are in excellent agreement with (a) the entrance thermal region for a zero yield (Newtonian fluid), and (b) the fully developed temperature distributions for all yield and marginal layer thickness numbers, it can be assumed that the results obtained are accurate to within the limits of the discretization error due to the grid size.

It is pointed out that also in the thermal inlet region with fully developed flow the existence of a plug flow region is responsible for the increase of the heat transfer rate.

Checking two sets of results referring to different rheological models, it is observed that for all Y and D numbers a more refined model damps the plug flow

region so that the increase in Nusselt number is reduced.

The presence of a thin Newtonian fluid layer at the wall enhances the width of the plug flow region and the effect on the heat transfer coefficients is comparable with the one due to an increase in yield number.

Acknowledgements The authors would like to thank Professor S. Salvigni for helpful remarks during the revision of the paper. Financial support was given by C.N.R. (Consiglio Nazionale delle Ricerche), Grant No. 80.01224.07.

REFERENCES

1. D. O. Cooney, *Biomedical Engineering Principles: an Introduction to Fluid, Heat, and Mass Transport Processes*. Marcel Dekker, New York (1975).
2. S. Charm and G. S. Kurland, Viscometry of human blood for shear rates 0–100,000 sec^{-1}, *Nature, London* **206,** 617–619 (1965).
3. E. W. Merrill and G. A. Pelletier, Viscosity of human blood: transition from Newtonian to non-Newtonian, *J. Appl. Physiol.* **23,** 179–182 (1967).
4. E. W. Merrill, A. M. Benis, E. R. Gilliland, T. K. Sherwood and E. W. Salzman, Pressure-flow relations of human blood in hollow fibres at low flow rates, *J. Appl. Physiol.* **20,** 954–967 (1965).
5. S. Salvigni, M. Mariotti and G. S. Barozzi, Determinazione delle perdite di carico e dei profili di velocità medi nell'apparato circolatorio, *Atti Accad. Sci. Ist. Bologna* **265,** 135–155 (1977).
6. V. Mitvalsky, Heat transfer in laminar flow of human blood through tube and annulus, *Nature, London* **4981,** 307 (1965).
7. S. Charm, B. Paltiel and G. S. Kurland, Heat-transfer coefficients in blood flow, *Biorheol.* **5,** 133–145 (1968).
8. S. Victor and V. L. Shah, Heat transfer to blood flowing in a tube, *Biorheol.* **12,** 361–369 (1975).
9. S. Victor and V. L. Shah, Steady state heat transfer to blood flowing in the entrance region of a tube, *Int. J. Heat Mass Transfer* **19,** 777–783 (1976).
10. S. V. Patankar and D. B. Spalding, *Heat and Mass Transfer in Boundary Layers*. Intertext, London (1970).
11. E. Zanchini, M. Mariotti and S. Salvigni, Heat transfer in circulatory system, *Rass. Bioing.* **4,** 33–44 (1979).
12. G. S. Barozzi and A. Dumas, Un metodo numerico di soluzione di problemi assialsimmetrici di scambio termico laminare, *Quad. Ist. Fisica Tecnica*. Patron, Bologna (1980).
13. A. Dumas and G. S. Barozzi, Laminar flow heat transfer with axial conduction in a circular tube: a finite difference solution, in *Numerical Methods in Thermal Problems* (edited by R. W. Lewis, K. Morgan and B. A. Schrefler), Vol. 2, pp. 1111–1121. Pineridge Press, Swansea (1981).
14. J. Stoer, *Introduzione all'Analisi numerica*, Vol. 1. Zanichelli, Bologna (1975).
15. W. McGuire and R. H. Gallagher, *Matrix Structural Analysis*. Wiley, New York (1979).
16. R. K. Shah and A. L. London, *Laminar Flow Forced Convection in Ducts*. Academic Press, New York (1978).

CONVECTION THERMIQUE LAMINAIRE POUR UN ECOULEMENT DE SANG DANS UN TUBE CIRCULAIRE

Résumé—On étudie la convection thermique en région d'entrée pour du sang qui coule en régime permanent dans un tube. On suppose que le comportement non-Newtonien du sang peut être exprimé à la fois par l'équation de Casson et la loi plus compliquée suggérée par Merrill et Pelletier [*J. Appl. Physiol.* **23,** 177–182 (1967)]. La possible présence d'une couche de plasma sans cellule à la paroi est considérée. La distribution de vitesse est déterminée analytiquement et une solution de l'équation de l'énergie est obtenue par une méthode aux différences finies pour deux cas: (a) température uniforme à la paroi et (b) flux thermique uniforme à la paroi. Des résultats sont présentés pour le nombre $Y\ (= 2R\tau_v/\sigma u_m)$ égal à 1, 5, 10 et 20 et l'épaisseur adimensionnelle de la couche marginale $D\ (= \delta/R)$ est égale à 0, 0,0002, 0,01 et 0,1.

DER WÄRMEÜBERGANG AN LAMINAR STRÖMENDES BLUT IN EINEM KREISRUNDEN KANAL

Zusammenfassung—Der Wärmeübergang im Einlaufbereich an gleichförmig strömendes Blut in einem Rohr wurde untersucht. Es wurde angenommen, daß das nichtnewton'sche Verhalten von Blut sowohl durch die Casson-Gleichung als auch das komplexe Gesetz von Merrill und Pelletier [3] ausgedrückt werden kann. Das mögliche Vorhandensein einer dünnen, zellfreien Plasmaschicht an der Wand wurde berücksichtigt. Die Geschwindigkeitsverteilung wurde analytisch bestimmt und eine Lösung der Energiegleichung durch eine finite Differenzenmethode für die beiden Fälle: (a) konstante Wandtemperatur und (b) konstanter Wärmestrom an der Wand, ermittelt. Ergebnisse werden für Fließ-Zahlen $Y = (2R\tau_y/\sigma u_m) = 1; 5; 10$ und 20 und für die dimensionslose Randschichtdicke $D = \delta/R = 0; 0{,}0002; 0{,}01$ und 0,1 angegeben.

ЛАМИНАРНЫЙ ТЕПЛОПЕРЕНОС К ПРОТЕКАЮЩЕМУ В КРУГЛОЙ ТРУБЕ ПОТОКУ КРОВИ

Аннотация—Исследуется теплоперенос во входной области при стационарном течении крови в трубе. Неньютоновские свойства крови описываются уравнением Кессона и более сложным законом, предложенным Мерриллом и Пелтье [*J. Appl. Physiol.* **23**, 179–182 (1967)]. Учитывается также возможность нахождения на стенке тонкого бесклеточного слоя плазмы. Распределение скорости определяется аналитически, а уравнение энергии решается конечно-разностным методом для двух случаев: (а) однородной температуры стенки и (б) однородного теплового потока на стенке. Результаты получены для значений чисел текучести $Y(=2R\tau_y/\sigma u_m) = 1, 5, 10$ и 20 и безразмерных толщин пограничного слоя $D(=\delta/R) = 0; 0{,}0002; 0{,}01$ и 0,1.